Bending Performance of Cross-laminated Timber-concrete Composite Slabs According to the Composite Method

Seung-Youp Baek, Yo-Jin Song, Seok-Hoon Yu, Dong-Hyeon Kim, and Soon-Il Hong *

Bending strength tests were conducted of cross-laminated timber (CLT)-concrete composite slabs according to the shear connection method and carbon fiber reinforced plastic (CFRP) reinforcement. The bending strength of the composite slab that was shear-connected with an epoxy adhesive was 17% higher than that of a composite slab that was shear-connected with a self-tapping screw. In addition, the CLT-concrete slip of the former composite slab was also measured as 20% lower than the latter under the same load, showing a behavior close to that of a full composite. Both shear connection methods generated a failure in a low load-deformation section when there was a defect in the outermost tensile laminae of the CLT. In contrast, the CFRP reinforcement in the tension part of the composite slab suppressed the failure at the defect in the outermost tensile laminae. This reinforcement effect increased the reliability of the bending performance of the composite slab by preventing the failure of the composite slab while in a constant failure mode. Furthermore, the slip of the composite slab decreased 49% after its reinforcement with CFRP, showing a behavior close to that of a full composite.

Contact information: Department of Forest Biomaterials Engineering, Kangwon National University, 1- Kangwondaehak-gil, ChunCheon-si, Gangwon-do, 24341, Republic of Korea;
 * Corresponding author: hongsi@kangwon.ac.kr

INTRODUCTION

The timber-concrete composite (TCC) first appeared in a bridge in the United States in the 1920s. In Europe, TCC was introduced as an alternative to steel concrete structures due to the lack of steel bars during the Second World War (Rodrigues *et al.* 2013). Recently, interest in timber, an environment-friendly material, has increased in the construction market, prompted in part by the rising temperature of the earth due to the increase in greenhouse gases, including carbon dioxide (Collins 2020). In particular, the emergence of cross-laminated timber (CLT), which is suitable for high-rise timber structures, is increasing the use of TCC combined with concrete. In the composite fabrication process of TCC, it is crucial to generate full composite behavior for loads by integrating CLT and concrete with different properties. A full composite refers to a case where there is no slip between two materials. When a behavior close to that of a full composite appears, the bending stiffness increases due to the small values of slip and deflection. In contrast, when two materials are not shear-connected, they are called a "no composite." When a behavior close to that of a no composite appears, the bending stiffness decreases due to the occurrence of a large slip and a large deflection (Fragiacomo and Lukaszewska 2011). In the TCC field, a composite fabrication process that shear-connects two materials using a

physical or chemical method is being researched. Screws are mainly used for the physical connection methods.

In a study by Park and Lee (2019), the maximum load was highest when a shear connector was inserted into a CLT at 90°; a shorter depth of the insertion of the shear connector into the concrete resulted in more concrete failure and the nail pull-out phenomenon occurred (Park and Lee 2019). However, Kim and Kim (2018) found that when the insertion angle was 90°, the lowest maximum shear strength and the slip modulus were obtained, and the shear performance was highest at the insertion angle of 45°. Mai *et al.* (2018) confirmed that the bending stiffness (EI) of bending specimens was highest and the slip was smallest when the screw insertion angle was 45°. Thus, it has been verified that the bending performance of TCC is highest when the connector insertion angle is 45°. Besides the frequently used screws, steel plates such as mesh plates (Mudie *et al.* 2019) and hot-galvanized steel plates (Estévez-Cimadevila *et al.* 2020) have been developed. Furthermore, Lukaszewska *et al.* (2010) performed various composite fabrication processes, such as insertion of screws in a steel tube, use of ring-shaped nails in steel plates, and insertion of screws in the notch joint and the steel tube. Studies on composite fabrication processes using screws and notches together have also been conducted (Jorge *et al.* 2010; Jiang and Crocetti 2019). Methods that use adhesives as chemical connectors besides metal shear connectors have also been studied. Brunner *et al.* (2007) developed a special adhesive that can bond CLT with wet or hardened concrete (Brunner *et al* 2007). Song *et al.* (2021) raised the problem of the degradation of the quality of CLT due to the moisture of the concrete when a CLT-concrete composite slab is fabricated with a shear joint, and they found that such problems could be solved using a shear connection method with epoxy adhesive. Excellent single shear performance and bending performance of the structural lumbers are obtained by shear-connected timber and concrete by using a self-tapping screw (STS) and epoxy adhesive (Tannert *et al.* 2020). The bending performance of TCC is being researched according to various compounding methods. However, few studies have been conducted on the slip between CLT and concrete and bending stiffness. Such studies could indicate the full composite performance according to the shear connection method, which is important in composite floor plates. Therefore, differences in the degree of full composite and bending stiffness need to be researched by investigating the slip of TCC slabs according to the shear connection method.

Not only the composite fabrication process using the shear connection method but also methods that attach reinforcements such as fiber-reinforced plastic (FRP) can be used in the composite fabrication process of CLT-concrete composite slabs. Hence, studies have been conducted on the composite fabrication process for CLT and FRP to improve the bending performance of CLT. When the tensile laminae of CLT was reinforced with glass fiber-reinforced plastic sheets, the modulus of elasticity (MOE) and the modulus of rupture (MOR) increased 7% and 17% from those of the CLT, respectively (Song and Hong 2018). Furthermore, Song *et al.* (2019) reinforced CLT with carbon fiber-reinforced plastic (CFRP) in the form of a sheet and a rod. The MOE and MOR of the CLT reinforced with the sheet increased 27% and 48% from those of the CLT, respectively, and the MOE and MOR of the CLT reinforced with a rod increased 9% and 8% from those of the CLT, respectively. Therefore, it is believed that CLT will show a high bending performance when the tensile laminae of the CLT of a CLT-concrete composite slab is reinforced with a CFRP sheet.

This study also assessed the bending performance of a CLT-concrete composite slab fabricated using the shear connection method and CFRP reinforcement. In addition,

the bending strength value was predicted using the gamma method and compared with the experimental value.

EXPERIMENTAL

Materials

CLT and concrete

       The CLTs were fabricated with domestic *Larix kaempferi* Carr. laminae. The average air-dry specific gravity of the laminae was 0.54 ± 0.04, and the average air-dry moisture content was $12 \pm 1.1\%$. The MOE of the laminae was measured using a non-destructive method *via* the natural frequency of the longitudinal vibration, and the measured MOE of the laminae was classified in accordance with KS F 3021 (2013). The MOE of the laminae of the major direction (longitudinal direction) comprising the CLT was 13.1 GPa, and the MOE of the transverse direction was 10.7 GPa. Phenol-resorcinol formaldehyde (PRF) was used for inter-laminar adhesion by applying 400 g/m^2 of it on one side with 1.0 MPa pressure (Song and Hong 2016). The design strength of the concrete was 24 MP. For the concrete fabrication, Portland cement (Cheonmapyo cement, Sungshin Cement Co., Ltd., South Korea) and coarse aggregates with the maximum size of 25 mm were used. The water/cement ratio of the concrete for the mix design was 0.43.

Slab production according to the shear connection method and CFRP reinforcement

       The Type-A specimen was fabricated as a 5-ply CLT with a length of 3,000 mm, a width of 240 mm, and a height of 150 mm (Figs. 1 and 2). The Type-B specimen was fabricated by pouring wet concrete to up to 60 mm thick over a 90 mm-thick CLT. Self-tapping screw (ASSAY 3.0 SK, Wurth, Germany) was used for the shear connection between the CLT and the concrete. The joint with an STS was designed with an end distance of 18D (D: diameter of the STS), an edge distance of 5D, an 18D space between the rows of bolts, and a 5D space between the bolts in a row (ETA 11/0190 2013). The STSs were inserted in 14 lines of four units at an insertion angle of 45° (Kim and Kim 2018) and an insertion depth of 10D.
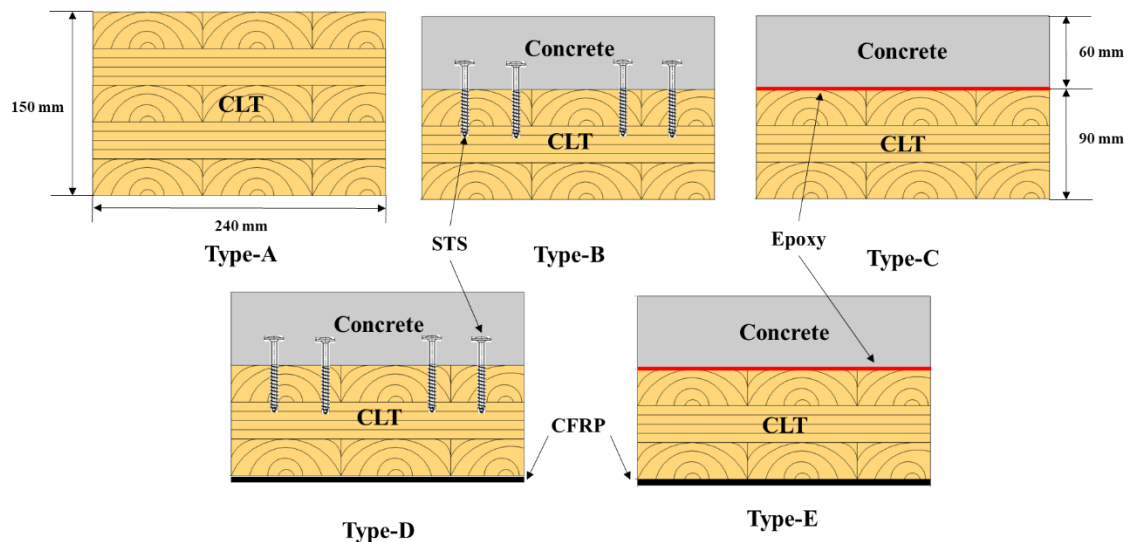

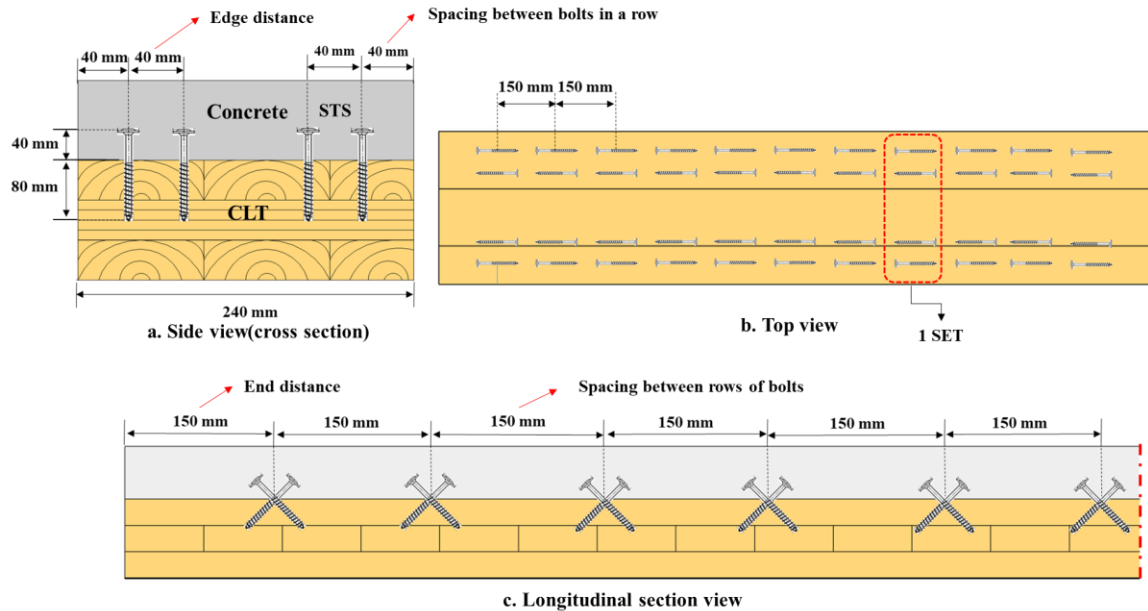**Fig. 1.** Schematic of specimens using shear connection and CFRP reinforcement (cross-section)

Fig. 2. STS design method and schematics of the specimens in each direction of shear-connected with the STS (Type-B and Type-D)

The Type-C specimen was fabricated by pouring wet concrete to up to 60 mm thick before the epoxy adhesive (Sikadure 31, Sheet, S. P. D, Sika, Switzerland), which had been applied over the CLT to 1.0 mm thick, had hardened. The Type-D specimen was fabricated using the same shear connection method as that used for the Type-B specimen, by reinforcing the entire surface of the CLT tensile lamina with a 1.2 mm-thick CFRP sheet (Shinsung Materials, Seoul City, South Korea). The MOE and the tensile strength of the CFRP used were 470,000 and 2557 MPa, respectively (Park *et al*. 2009). A polyurethane adhesive (OTTO COLL P84, Otto, Germany) was used to bond the CLT and the CFRP by applying 300 g/m^2 of it on one side at a pressure of 1.0 MPa (Song *et al.* 2019). The Type-E specimen was fabricated by shear-connecting the epoxy CLT and the concrete with an adhesive and reinforcing them with CFRP. Two specimens were fabricated for each type. After the concrete was poured, it was cured at room temperature for 40 days.

Methods

Bending strength test

A bending strength test was performed with a 4-point load in three divisions, as shown in Fig. 3.
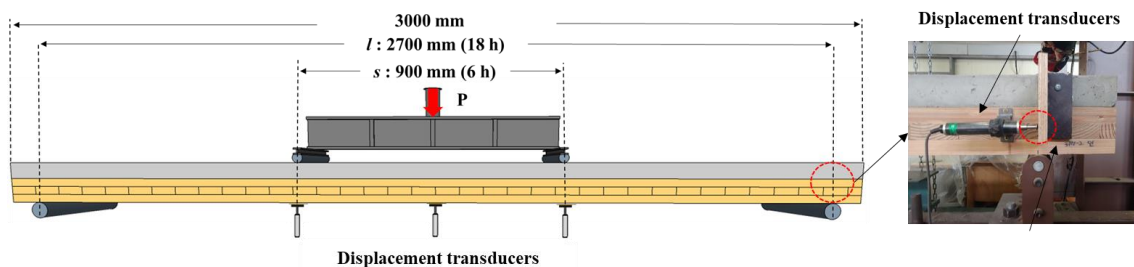

Fig. 3. Set up for bending strength measurement of the slip between the CLT and the concrete

The span-to-depth ratio was 18:1, the distance between the two loading points was 6 times the depth of the specimen, and the loading rate was 5 mm/min as per BS EN 16351 (2015). To measure the deflection of the specimens, displacement meters (CDP-50, Tokyo Sokki Kenkyujo, Tokyo, Japan) with a maximum capacity of 50 mm were installed at the center of each specimen (global) and at each loading point (local). The slip between the concrete and the CLT was measured using a displacement meter (CDP-25, Tokyo Sokki Kenkyujo, Tokyo, Japan) with a maximum capacity of 25 mm installed at the CLT after fixing a tip fabricated for slip measurement to the concrete.

RESULTS AND DISCUSSION

Load-deflection Curve and Failure Mode

Both specimens of Type-A, a 5-ply CLT, formed a straight-line section in the load-deformation graph (Fig. 4).
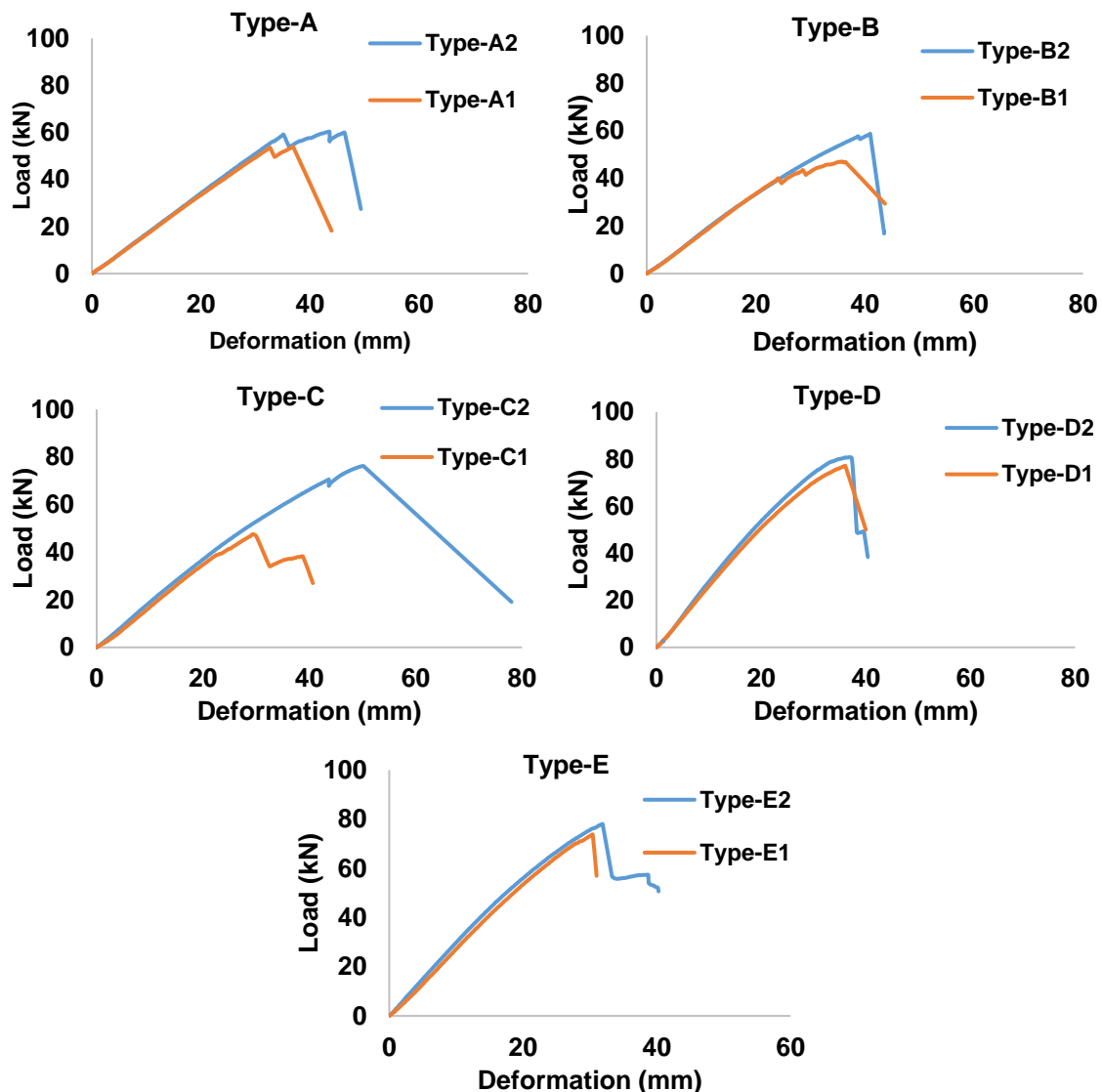

Fig. 4. Load-deflection curves from the static bending test

Then, as shown in Fig. 5, the first failure occurred in the tensile lamina of the CLT, and the final rolling shear failure occurred in the middle lamina. CLTs are usually fractured at defects such as knots in the outermost tensile lamina or undergo rolling shear failure along the annual ring in laminated timber (Song 2017).
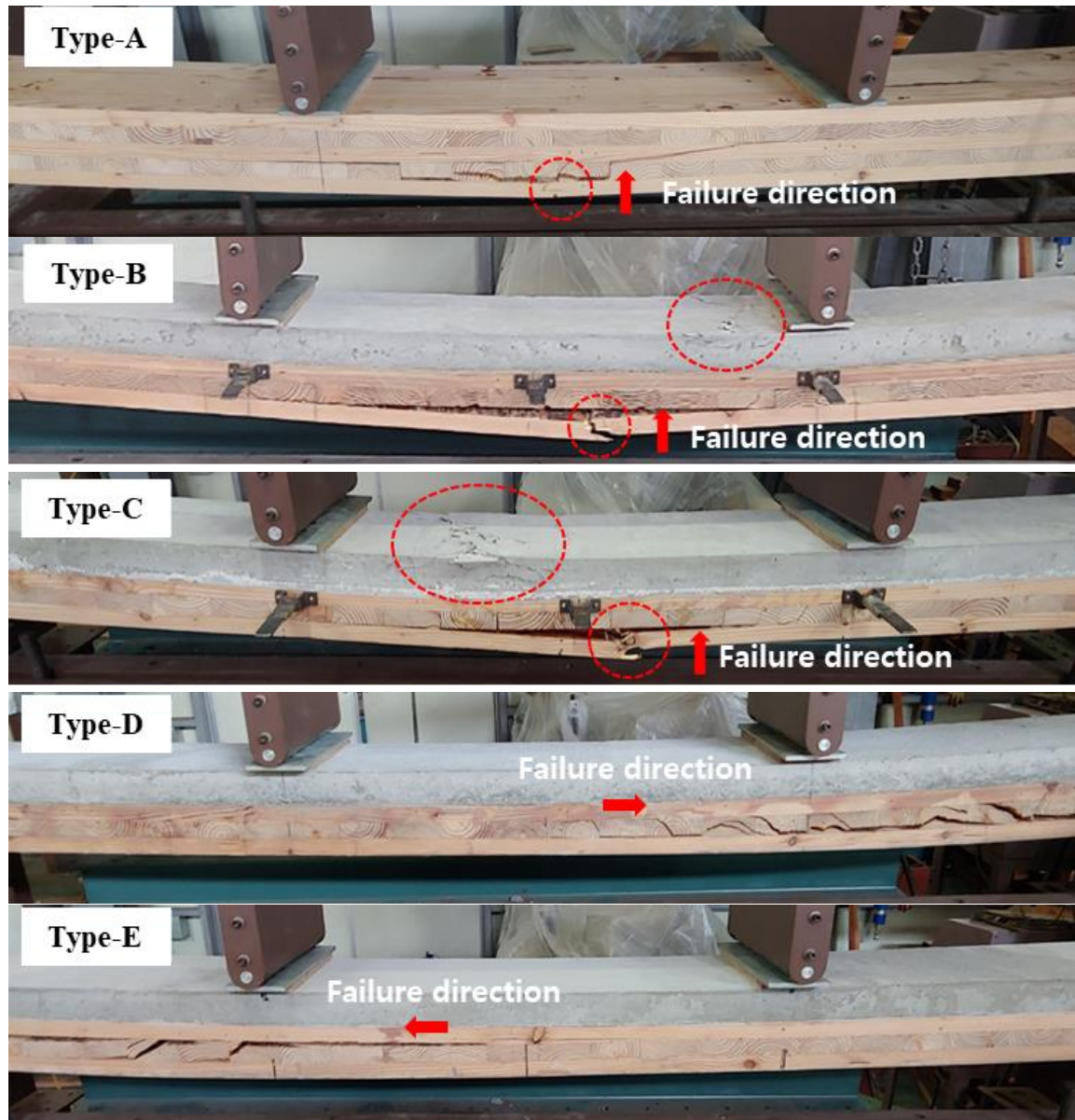

Fig. 5. Photographs of the failure directions and modes of the specimens from the bending strength tests (Type-A: tensile failure, Type-B: tensile failure, Type-C: tensile failure, Type-D: rolling shear failure, and Type-E: rolling shear failure)

It was found that the maximum load of Type-C2 was 76.2 kN; thus, it endured the maximum load of the composite floor plate reinforced with CFRP. However, the maximum loads of Type-B1 and Type-C1 were lower by 25% and 38% than those of Type-B2 and Type-C2, respectively. The reason for this was the presence of knots in the outermost tensile lamina of Type-B1 and Type-C1 unlike Type-B2 and Type-C2, and failure occurred

in a low load-strain section due to these knots. Ján Kanócz and others who examined failure mode according to the shear connection method of CLT-concrete composite floor plates also reported that failure occurred in the outermost tensile lamina of CLT regardless of the shear connection method Ján Kanócz 2013, 2014, 2015), particularly at defects such as knots (KQ *et al.* 2018). These results confirmed that the defects in the outermost tensile lamina of the CLT decreased the bending performance of a composite slab, regardless of the shear connection method.

In contrast, for the reinforced Type-D and Type-E specimens, the tensile failure was suppressed by the CFRP despite the presence of a knot in the outermost tensile lamina, and the specimens had a certain failure mode by the rolling shear through the suppression of the tensile failure.

Unlike the tensile failure of glulam reinforced with CFRP sheets (Glišović *et al.* 2017), reinforced TCCs are more vulnerable to shear strength rather than tensile failure. Thus, it was found that rolling shear failure occurred along the annual ring of the laminated timber in the direction perpendicular to the fiber. This failure mode decreased the maximum load deviation of the composite slab by a factor of 5. In addition, the maximum load of the slabs reinforced by the CFRP increased 34% compared to that of the slab that was not reinforced by the CFRP.

Meanwhile, there was no difference of local deflection ratio to the global deflection by the shear connection method of the CLT-concrete composite specimens. The CFRP-reinforced slab was less affected by the shear force because the ratio of its local deflection to the global deflection was lower than that of the slab that was not reinforced with CFRP.

Table 1. Bending Test Results

Specimens		Moisture Content (%)	Max. Load (kN)	Ave. M. Load (kN)	Global Deflection (mm)	Ave. Global Deflection (mm)	Local Deflection (mm)	Ave. Local Deflection (mm)	Global Deflection or Local Deflection
Type-A	1	13.4	53.1	56.1	36.9	36.0	34.2	32.9	1.09
	2	11.5	59.1		35.1		31.7		
Type-B	1	12.8	47.1	53.0	35.8	38.4	33.3	34.8	1.10
	2	12.5	58.8		41.1		36.6		
Type-C	1	11.7	47.5	61.9	29.5	39.8	26.9	36.0	1.10
	2	12.6	76.2		50.2		45.2		
Type-D	1	11.6	77.2	78.9	36.1	36.1	33.7	34.1	1.05
	2	12.3	80.7		36.1		34.6		
Type-E	1	12.9	73.8	75.9	30.3	31.1	28.7	29.4	1.05
	2	10.7	78.0		31.9		30.1		

Bending Performance and Composite Action

The MOE of Type-B was 2% higher than that of Type-A, but the MOR of Type-B was 5% lower than that of Type-A. The MOE and MOR of Type-C were 4% and 17% higher than those of Type-B, respectively. The slips under the same load condition were less than 1.0 mm for both Type-B and Type-C specimens, but the slip of Type-C was 80% lower than that of Type-B. The slab that was shear-connected with an epoxy adhesive showed a higher MOR than the slab that was shear-connected with an STS and showed a behavior close to that of a full composite because the slip was low. Joakim Thilén also reported that the slip of the TCC slab was 0.01 to 0.02 mm in adhesive shear connection and 0.23 to 0.27 mm in the notch+STS junction. Thus, the adhesive shear connected TCC slab was closer to full composite and its bending stiffness was 12% higher as well (Joakim 2017).

The average MOE and MOR of the CFRP-reinforced slab were 59% and 26% higher than those of the slab that was not reinforced. Song *et al.* (2019) found that when CLT was reinforced with CFRP sheets, the MOE and MOR increased by 27% and 48% compared to CLT, respectively. When the bending performance is compared between the CFRP-reinforced CLT and composite floor plates, the MOR of the CLT-concrete composite floor plate improved greatly owing to the CFRP reinforcement, but the increase rate was lower than that of the single CLT reinforced with CFRP. However, the MOE of the CFRP-reinforced composite floor plate was much higher than that of CLT because the concrete endured compression and the CLT endured tension.

Regarding the slip under the same load condition (47 kN) of the CLT-concrete composite slab that was shear-connected with STS, the slip of the CFRP-reinforced slab was 43% lower than that of the slab not reinforced with CFRP. Regarding the slip of the slabs that were shear-connected with epoxy adhesive under the same load, the slip of the CFRP-reinforced slab was 55% lower than that of the non-CFRP-reinforced slab. The slips of the CLT-concrete composite slabs reinforced by CFRP decreased in both shear connection methods, showing a behavior close to that of a full composite. The CLT-concrete composite slab reinforced with CFRP did not show differences in bending performance using the shear connection method. Regarding the slip of the CFRP-reinforced CLT-concrete composite slab, the slip of Type-D was 6.3 times higher than that of Type-E. This confirmed that the bending performance also increased as the slip decreased.

Table 2. Bending Properties of the CLT and the CLT-concrete Composite Slabs

Specimens	MOE$_{Global}$ (MPa)	MOE$_{Local}$ (MPa)	MOR (MPa)	Max. Slip (mm)	Slip at 47 kN (mm)
Type-A	8,747	9,271	32.7	-	
Type-B	8,921	9,456	30.9	0.81	0.66
Type-C	9,269	9,829	36.1	0.16	0.13
Type-D	14,317	15,176	46.0	1.44	0.38
Type-E	14,429	15,259	44.3	0.11	0.06

MOE$_{Global}$: Modulus of elasticity determined by the global deflection; MOE$_{Local}$: modulus of elasticity determined by the local deflection; and MOR: modulus of rupture

Bending performance prediction design using the Gamma method

When the CLT and the concrete were shear-connected using STS, $r_i = [1 + \pi^2 E_i A_i s / K L^2]^{-1}$ was used. For the slip modulus of the STS, 31.2 kN/mm was used, which was measured using the same STS as that in a previous study (Gerber 2016). As for K, 124.8 kN/mm was applied, which is the sum of the slip moduli of four STSs, because it was designed with one set of four STSs, as shown in Fig. 3. Furthermore, when the CLT was bonded with other materials using an adhesive, $r_i = 1$ was applied. In this study, the rolling shear modulus G_r was calculated based on the *CLT Handbook* (Gagnon and Pirvu 2011). For the reference bending strength (F_b) value in the bending moment design, 50 MPa was used (Hwang *et al.* 2011).
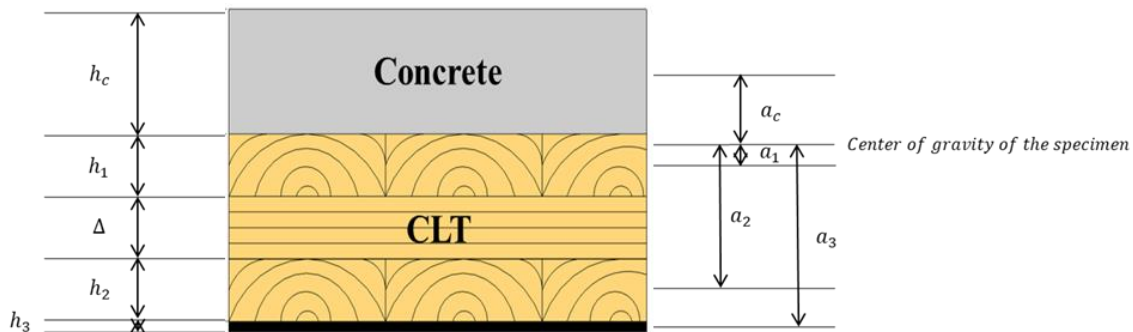

Fig. 6. Cross-section of the CLT-concrete composite slab reinforced with CFRP

Bending stiffness (*EI*) was calculated according to Eq. 1,

$$EI_{\text{eff}} = \sum (E_i I_i + \gamma_i E_i A_i a_i^2) \tag{1}$$

where EI_{eff} is bending stiffness (EI) by the Gamma method (kN·m^2); E_i denotes MOE of the panel (MPa); I_i is effective moment of the inertia of layer I (mm^4); I is geometrical moment of the inertia (mm^4); A represents cross-section (mm^2); h_i stands for thickness of layer i (mm); a_i is the distance between the central axis of each panel (mm); and γ denotes connection efficiency factor ($0 < \gamma \leq 1$);

Distance between the central axis of each panel (a_i) was calculated according to Eqs. 2 through 5,

$$a_c = \frac{h_c + h_1}{2} - a_1 \tag{2}$$

$$a_1 = \frac{r_c E_c A_c \left(\frac{h_c}{2} + \frac{h_1}{2}\right) - r_2 E_2 A_2 \left(\frac{h_2}{2} + \frac{h_1}{2} + \triangle\right)}{\sum r_i E_i A_i} \tag{3}$$

$$a_2 = a_1 + \frac{h_1}{2} + \frac{h_2}{2} + \triangle a_1 \tag{4}$$

$$a_3 = a_2 + 0.6 + \frac{h_2}{2} \tag{5}$$

where Δ is thickness of transverse layer (mm).

The factor γ is depend on the shear behavior of transverse layer and can be expressed as Eq. 6,

$$\gamma_i = \frac{1}{1+\pi^2 \frac{E_i A_i}{l^2} \frac{\triangle}{G_r b}} \qquad (6)$$

where G_r is rolling shear modulus (MPa); l is span (mm)

Bending moment (M) was calculated according to Eq. 7,

$$\boldsymbol{M = \emptyset \cdot f_b \cdot \frac{(EI)_{eff}}{E_i(\gamma_i a_i + 0.5 h_i)}} \qquad (7)$$

where ϕ is resistance factor (0.9); and f_b represents bending strength (MPa).

The difference between the bending stiffness value predicted by the Gamma method and the measured value was 4.3% on average, and the maximum prediction error was 7.9%. Type-B and Type-C showed measured values higher than predicted values. As for Type-D to Type-E, the predicted values were lower than the measured values. The average difference between the predicted and measured values of the bending moment was 7.0%. Both Type-B and Type-C not reinforced with CFRP showed high measured values. Type C showed an error of 14.6% and the measured values were higher. It seems that the maximum load of Type-C2 was measured high, resulting in a large difference between predicted and measured values. In the case of the CFRP-reinforced composite floor plates, different values were predicted depending on the shear connection method. The maximum bending moment of Type-D was higher than the predicted value, but the predicted value was higher than the measured value for Type-E.

Table 3. Comparison of the Predicted and Measured Bending Performance Values

Specimens	EI_{Test} (kNm²)	EI_{Gamma} (kNm²)	EI_{Gamma}/EI_{Test} (%)	Mb_{Test} (kNm)	Mb_{Gamma} (kNm)	M_{Gamma}/M_{Test} (%)
Type-A	590	585	-0.9	28.0	30.5	8.9
Type-B	602	610	1.3	26.5	26.1	-1.6
Type-C	625	672	7.5	30.9	26.5	-14.6
Type-D	966	890	-7.9	39.5	37.3	-5.6
Type-E	974	937	-3.8	38.0	39.7	4.4

EI_{Test}: Bending stiffness determined by the static bending test; EI_{Gamma}: Bending stiffness determined by the Gamma method; Mb_{Test}: Bending moment determined by the static bending test; and Mb_{Gamma}: Bending moment determined by the gamma method

CONCLUSIONS

1. The modulus of elasticity (MOE) of the cross-laminated timber- (CLT)-concrete composite slab that was shear-connected with epoxy adhesive did not remarkably vary from that of the slab connected with self-tapping screw (STS), but the modulus of rupture (MOR) of the former was somewhat high and the slip between the CLT and the concrete was low. Hence, it showed a behavior close to that of a full composite.

2. When there was a knot in the outermost tensile lamina of the CLT, the slab failed in the low load-deformation section regardless of the shear connection method, which resulted

in a large strength deviation.

3. The failure of the CLT-concrete composite slab reinforced with carbon fiber reinforced plastic (CFRP) was suppressed by the CFRP even when there was a defect in the outermost tensile lamina. As a result, it showed a constant failure mode from the rolling shear and a low strength deviation.

4. The values of the bending stiffness predicted by the Gamma method were almost consistent, but the predicted values of the bending moment were not consistent due to large errors.

ACKNOWLEDGEMENTS

REFERENCES CITED

Brunner, M., Romer, M., and Schnüriger, M. (2007). "Timber-concrete-composite with an adhesive connector (wet on wet process)," *Materials and Structures* 40(1), 119-126. DOI: 10.1617/s11527-006-9154-4

BS EN 16351 (2015). "Timber structures – Cross laminated timber – Requirements," The British Standards Institution, London, UK.

Collins, L. (2020). *Timber-Concrete Composite: An Alternative Composite Floor System*, Ph.D. Dissertation, Kansas State University, Manhattan, KS, USA.

Estévez-Cimadevila, J., Otero-Chans, D., Martín-Gutiérrez, E., and Suárez-Riestra, F. (2020). "Testing of different non-adherent tendon solutions to reduce short-term deflection in full-scale timber-concrete-composite T-section beams," *Journal of Building Engineering* 31, Article ID 101437. DOI: 10.1016/j.jobe.2020.101437

ETA 11/0190 (2013). "Würth self-tapping screws," European Technical Approval, German Institute for Building Technology, Queen Chelsea, Germany.

Fragiacomo, M., and Lukaszewska, E. (2011). "Development of prefabricated timber–concrete composite floor systems," *Proceedings of the Institution of Civil Engineers-Structures and Buildings* 164(2), 117-129. DOI: 10.1680/stbu.10.00010

Gagnon, S., and Pirvu, C. (2011). *CLT Handbook: Cross-laminated Timber*, FPInnovations, Quebec City, Canada.

Gerber, A. R. (2016). *Timber-Concrete Composite Connectors in Flat-Plate Engineered Wood Products*, Ph.D. Dissertation, University of British Columbia, British Columbia, Canada. DOI: 10.1061/9780784479117.201

Glišović, I., Pavlović, M., Stevanović, B., and Todorović, M. (2017). "Numerical analysis of glulam beams reinforced with CFRP plates," *Journal of Civil Engineering and Management* 23(7), 868-879. DOI: 10.3846/13923730.2017.1341953

Hwang, K. H., Park, J. S., and Park, M. J. (2011). *Evaluating Structural Performance of Graded Domestic Softwood Lumber*, Korea Forest Research Institute, Korea Forest Service, Seoul, Korea.

Jiang, Y., and Crocetti, R. (2019). "CLT-concrete composite floors with notched shear

connectors," *Construction and Building Materials* 195, 127-139. DOI: 10.1016/j.conbuildmat.2018.11.066

Jorge, L., Habenbacher, J., and Dujic, B. (2010). "Timber-concrete composite systems with cross-laminated timber," in: *Proceedings of 10th World Conference of Timber Engineering (WCTE)*, Trentino, Italy, pp. 1-8. DOI: 10.3403/bsiso16696

Kim, K. T., and Kim, J. H. (2018). "Load bearing capacity of CLT-concrete connections with inclined screws," *Journal of the Architectural Institute of Korea Structure and Construction* 34(4), 3-13. DOI: 10.5659/JAIK_SC.2018.34.4.3

KS F 3021 (2013). "Structural glued laminated timber – The Ministry of Knowledge Economy," Korean Agency for Technology and Standards, Seoul, Korea.

Lukaszewska, E., Fragiacomo, M., and Johnsson, H. (2010). "Laboratory tests and numerical analyses of prefabricated timber-concrete composite floors," *Journal of Structural Engineering* 136(1), 46-55. DOI: 10.1061/(asce)st.1943-541x.0000080

Mai, K. Q., Park, A., Nguyen, K. T., and Lee, K. (2018). "Full-scale static and dynamic experiments of hybrid CLT–concrete composite floor," *Construction and Building Materials* 170, 55-65. DOI: 10.1016/j.conbuildmat.2018.03.042

Mudie, J., Sebastian, W. M., Norman, J., and Bond, I. P. (2019). "Experimental study of moment sharing in multi-joist timber-concrete composite floors from zero load up to failure," *Construction and Building Materials* 225, 956-971. DOI: 10.1016/j.conbuildmat.2019.07.137

Park, A. R., and Lee, K. (2019). "Experimental and analytical study of shear connectors for the CLT-concrete composite floor system," *Journal of the Korean Association for Spatial Structures* 19(1), 65-73. DOI: 10.9712/KASS.2019.19.1.65

Park Jun-Chul, Shin Yoon-Jong, and Hong, S. I. (2009). "Bending performance of glulam beams reinforced with carbon fiber-reinforced plastics bonded with polyvinyl acetate-based adhesive," *J. Korean Wood Science and Technology* 37(4), 364-371.

Rodrigues, J. N., Dias, A. M., and Providência, P. (2013). "Timber-concrete composite bridges: State-of-the-art review," *BioResources* 8(4), 6630-6649. DOI: 10.15376/biores.8.4.6630-6649

Song, Y. J., Baek, S. Y., Lee, I. H., and Hong, S. I. (2021). "Variations of moisture content in manufacturing CLT-concrete composite slab using wet construction method," *BioResources* 16(1), 372-386. DOI: 10.15376/biores.16.1.372-386

Song, Y. J., and Hong, S. I. (2016). "Evaluation of bonding strength of larch cross-laminated timber," *Journal of the Korean Wood Science and Technology* 44(4), 607-615. DOI: 10.5658/WOOD.2016.44.4.607

Song, Y. J., and Hong, S. I. (2018). "Performance evaluation of the bending strength of larch cross-laminated timber," *Wood Research* 63(1), 105-115.

Song, Y. J., Lee, I. H., Song, D. B., and Hong, S. I. (2019). "Evaluation of delamination and bending performance of composite CLT reinforced with CFRP," *Wood and Fiber Science* 51(4), 1-10. DOI: 10.22382/wfs-2019-034

Tannert, T., Gerber, A., and Vallee, T. (2020). "Hybrid adhesively bonded timber-concrete-composite floors," *International Journal of Adhesion and Adhesives* 97, article ID 102490. DOI: 10.1016/j.ijadhadh.2019.102490